THE JOURNAL OF PHYSICAL CHEMISTRY B

ARTICLE

pubs.acs.org/JPCB

Surface Effects on the Demixing of Colloid−Polymer Systems

E. A. G. Jamie,* R. P. A. Dullens, and D. G. A. L. Aarts

Department of Chemistry, Physical and Theoretical Chemistry Laboratory, University of Oxford, South Parks Road, Oxford OX1 3QZ, United Kingdom

ABSTRACT: We studied the effect of a solid surface on the fluid−fluid phase separation of a colloid−polymer mixture in real space, exploring demixing from both the unstable and metastable regions of the phase diagram. The presence of a wall breaks the symmetry of the phase separation morphology in the direction perpendicular to the surface, influencing the coarsening behavior of domains. We analyzed the thickening of the wetting layers and found that hydrodynamic transport processes can significantly increase the rate of wetting-layer growth. Depending on the volume ratio between the two phases, a new regime was observed in which the demixing structure disconnected from the wall, but remained bicontinuous in the bulk. We also discuss the effect of a crossover in the demixing regime of bulk domains on the growth of this layer.

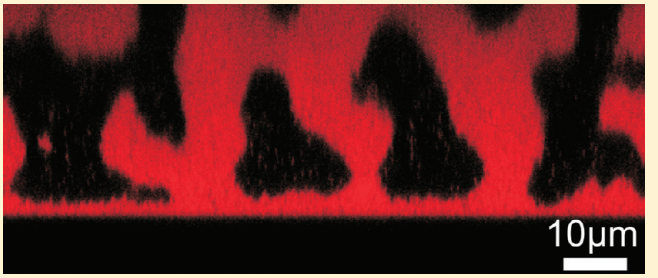

1. INTRODUCTION

The demixing of fluids has been extensively studied by both experimentalists and theoreticians for the past four decades.[1−3] The decomposition of a homogenized mixture leads to the development of complex patterns that coarsen as the system moves toward equilibrium. If these fluids are brought into the vicinity of a solid wall, the surface will have a preference for one of the phases over the other, leading to the buildup of a layer of the preferred phase on the surface. Upon equilibration, the strength of the interactions between the fluid phases and the surface is characterized by the contact angle between the fluid−fluid interface and the wall.[4] When an unstable mixture decomposes in the vicinity of a wetting surface, two different processes occur: bulk phase separation and wetting-layer growth. The surface field can have a dramatic effect on the evolving morphology[5] and results in different coarsening behaviors in the directions parallel and perpendicular to the wall, breaking the symmetry of the phase separation.[6−8] This phenomenon is known as surface-directed spinodal decomposition (SDSD) and is of considerable interest because a demixing sample will never be entirely free of surface effects, for example, due to the walls of its container or its interface with air.

When a two-phase system demixes in contact with a wetting surface, this surface will become the origin of an oscillating density wave. This wave propagates perpendicular to the surface into the bulk, breaking the symmetry of the domains.[6,7,9−11] For unstable fluid−fluid mixtures, this morphology consists of a wetting layer of the preferred phase on the surface and then a further (depletion) layer of the nonpreferred phase.[12] This can be followed by additional alternating layers moving toward the bulk, where the system separates through spinodal decomposition. In the proximity of the surface, the wavelength of the density oscillations coarsens with a power law; its amplitude decreases at greater distances from the surface, where the wave is destroyed by isotropic bulk fluctuations.[6,7,13] The distance that the wave penetrates the bulk is dependent on the strength of the surface field and the depth of the quench.[8,13−15] The presence of this density oscillation is likely to result in a difference in the physical length scales of domains parallel and perpendicular to the surface, although they coarsen according to the same power law with different prefactors quantifying their variation in size.[7,9,11]

Extremely off-critical systems from the metastable region of the phase diagram will separate through the nucleation and growth mechanism in the bulk. In the vicinity of a wetting surface, the layered morphology is similar to that observed in the spinodal case; however, the growth of the wetting layer occurs by a different process.[16−18] The extent to which the minority phase wets the surface leads to differences in the competition between the demixing and wetting processes, and therefore, different potential gradients drive the phase separation process.[16−18]

Depending on the strength of the preference of the surface for one phase or the other, the system will evolve into either a partially or a completely wet morphology.[4] The kinetics of the formation of this layer is determined by the competition between the bulk and the surface for the wetting phase, characterized by the size and range of the surface potential.[19,20] Hydrodynamic effects, which play an important role in the bulk spinodal decomposition of fluid−fluid mixtures,[21] have also been shown to accelerate wetting-layer growth in systems undergoing SDSD.[13,22−24]

In this article, we explore the domain morphologies and wetting-layer growth of colloid−polymer mixtures demixing in the presence of a completely wetting surface. The separation of a system of colloidal particles and nonadsorbing polymer into two

Received: July 29, 2011
Revised: September 27, 2011
Published: September 30, 2011

fluid phases is due to an attractive depletion interaction between the colloids, mediated by the polymers.[25,26] One phase is rich in colloids and poor in polymers and is known as a colloidal "liquid"; the other is rich in polymers and poor in colloids and is known as a colloidal "gas". Because of the larger size of the colloids, the interfacial tension in such a system is many orders of magnitude smaller than that in a molecular system, with the implication that the capillary length and interfacial roughness occur on the order of micrometers. This allows for the real-space observation of interfacial fluctuations[27] and their role in wetting-layer dynamics.[28,29] We first detail our experimental system and analysis method, before presenting our results. We then discuss our results in the context of previous observations before presenting our conclusions.

2. EXPERIMENTAL SYSTEM AND ANALYSIS

A dispersion of fluorescently labeled poly(methyl methacrylate) (PMMA) particles in water was prepared using the first part of the emulsion polymerization method described by Kumacheva et al.[31] The spherical colloidal particles, with a radius of R_c 110 nm, were characterized using scanning electron microscopy and found to be of low polydispersity, corroborated by the fact that samples spontaneously crystallized. A solution of xanthan polymer ($M_w = 4 \times 10^6$ g mol^{-1}, radius of gyration $R_g = 264$ nm) was prepared as described in ref 32. Combining these two components in the appropriate concentrations gives a fluid−fluid phase separating mixture with $q = R_g/R_c = 2.5$;[33] the experimental phase diagram of this system can be found in ref 34.

The solvent of a stock solution of colloids was converted into a mixture of approximately 23% water and 77% glycerol by repeated centrifugation, allowing the samples detailed in Table 1 to be prepared. By increasing the viscosity of the dispersing solvent, we decrease the rate at which phase separation progresses,[35] allowing the demixing of the system at a single wall to be observed in detail. This system of PMMA colloids and xanthan polymer dispersed in a glycerol−water mixture is discussed extensively in ref 35. The samples were homogenized using a vortex.

Bulk phase separations were recorded in real space using confocal scanning laser microscopy (CSLM; Zeiss Exciter) with a 10× magnification lens in the direction parallel to gravity and the cell wall. The samples were allowed to demix in glass cuvettes of small enough dimensions to avoid distortion of domains by solvent shear, but of sufficient width that the cell walls should have a minimal effect on the bulk phase separation characteristics.

The effects of a surface on the decomposition of the sample were studied by pipetting a drop of sample onto a glass slide positioned perpendicular to gravity and recording the phase separation with a 63× magnification lens. Demixing was imaged in both the *xy* plane (parallel to the glass surface) and the *xz* plane (perpendicular to the surface). These experiments were run for a relatively short length of time to avoid any inconsistency effects of solvent drying, gravitational forces, or finite droplet size.

The coarsening rate of the system in the *xy* plane was determined by performing two-dimensional discrete Fourier transforms on the CSLM images, as described in refs 35−37. The Fourier transforms were radially averaged to obtain the structure factor $I(k,t)$, where I is the intensity of the image and k is the wavevector. The wavevector at the maximum intensity $I_{max} \equiv I(k_{max},t)$ was obtained using a Gaussian fit. The correlation length in the system corresponds to $L = L_{image}/k_{max}$, where L_{image} is the image width and the coarsening rate in the system was obtained by plotting L against time.

Intensity profiles were constructed by taking the average intensity of each row of pixels in the image. This averaging is demonstrated in the *xz* plane image in Figure 1a, along the *x* and *z* directions (solid lines). The position of the wall in each frame

Table 1. Sample Details[a]

sample	ϕ_c	ϕ_p	solvent ratio glycerol/water	estimated $\Delta\rho_{(colloid-solvent)}$ (g/cm^3)	approximate phase composition, ϕ_L:ϕ_G	$n_{solvent}$[30]
1	0.086	1.778	76:24	−0.01	1:3	1.44
2	0.038	3.063	51:49	0.06	1:10	1.40
3	0.078	2.326	75:25	−0.01	1:8	1.44

[a] φ_c and φ_p denote the volume fractions of colloids and polymers. For polymers R_g is used in the calculation of its volume. $\Delta\rho$ denotes the density difference between colloids and solvent. φ_L and φ_G are the volume fractions of the colloidal liquid and gas phases after phase separation has completed. $n_{solvent}$ is the refractive index of the solvent.

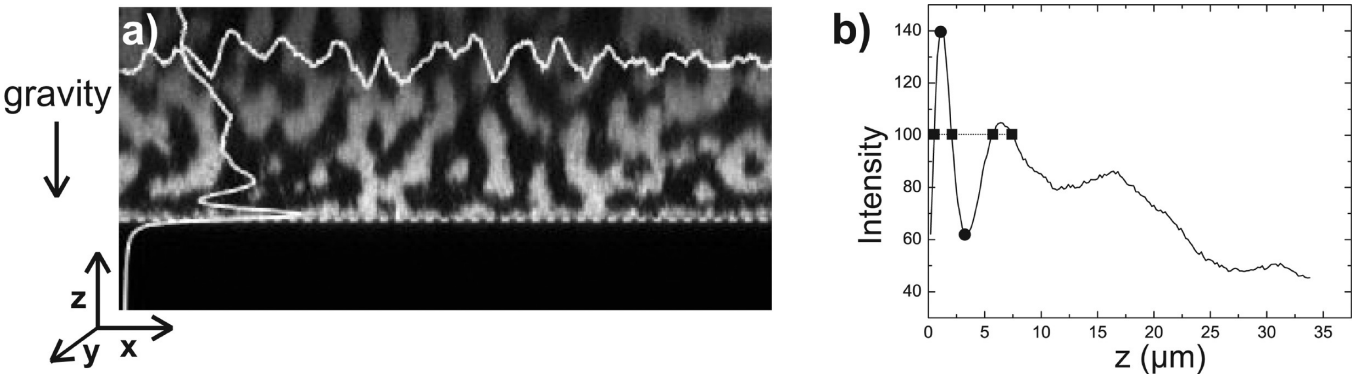

Figure 1. (a) Average intensity profiles across the *x* and *z* directions (solid lines). The dashed line represents the located position of the wall. (b) Intensity profile showing positions of relevant turning points (circles) and crossing points at the peak half-height (squares).

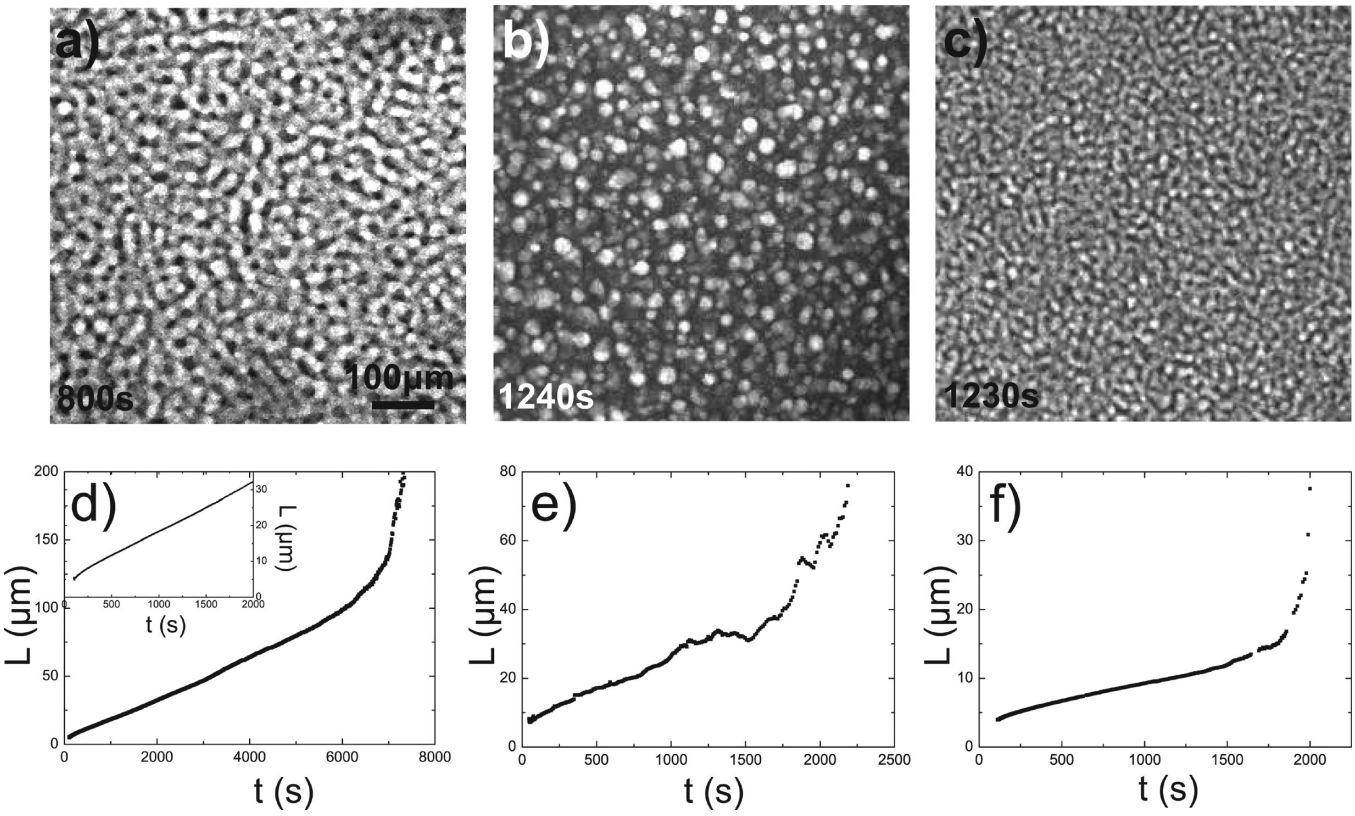

Figure 2. Bulk phase separations in the *xy* plane of samples (a) 1, (b) 2, and (c) 3. Growth of characteristic domain length scale L with time for samples (d) 1, (e) 2, and (f) sample 3. The inset in d shows growth at early times for sample 1.

was located by first binarizing the image and then averaging the image intensity in x to create an intensity profile in the z direction. The position of the wall was determined by finding the z coordinate location of the steepest gradient in the first peak of the profile and is denoted by the dashed line in Figure 1a.

The wetting-layer thickness was calculated by locating the positions of the turning points in the z direction intensity profile through numerical differentiation. The positions of these peaks are indicated in Figure 1b by black circles. The intensity value halfway between the first peak and trough was calculated and is denoted on the graph by a dashed line; the positions where the dashed line crosses the intensity profile were calculated and are marked by squares. The distance between the first two points where the dashed line and the intensity profile cross was taken as the average width of the wetting layer. The distance between the second and third points was taken as the average width of the depletion layer. It was not always possible to calculate the width of the depletion layer if the intensity of the second peak in the z profile was too low because of scattering by the colloidal particles. This effect leads to an overestimation of the depletion layer width, but we found this definition to be straightforward and workable. Additional distortion of the intensity profile is caused by the refractive index mismatch between the sample (see Table 1) and the immersion medium of the lens (n_{oil} = 1.51, Zeiss Immersol), leading to an elongation of the image. The image is stretched by a factor of n_{oil}/n_{sample}, leading to a lengthening of 6−8% in the direction of the z axis,[38] where we approximate the refractive index of the sample with that of the solvent. We corrected for this distortion when constructing intensity profiles in the direction perpendicular to the surface. Note that the measurement of the wetting-layer thickness is unreliable at early times, when it is comparable to the size of one pixel (0.2 μm), and at later times, if the width of any domains connected to the wetting layer becomes significant compared to the image width.

3. RESULTS AND DISCUSSION

Before considering the effect of a surface on the demixing of each sample, we establish the dynamics of demixing in the bulk (Figure 2). The CSLM images in Figure 2a−c show that samples 1 and 3 exhibit the classic spinodal network structure; upon equilibration, sample 3 contains a lower ratio of the liquid phase (Table 1). The demixing of sample 2 proceeds through nucleation and growth of droplets, which coarsen by coalescence with one another. We plot the development of the characteristic domain length scale L for each sample in Figure 2d−f. One can see that domains in the two spinodal samples grow in the linear hydrodynamic regime for the majority of the experiment; however, some curvature suggests the system might still be crossing over from the diffusive to the hydrodynamic regime at earlier times[35,39] (see Figure 2d,f). The length scale diverges as domains are ripped apart by buoyancy forces after around 6000 s for sample 1 and around 1500 s for samples 2 and 3. In samples 1 and 3, the density difference between the phases is such that the liquid phase rises, whereas in sample 2, the liquid phase sinks to the bottom of the container. We have not considered wetting-layer growth after the bulk demixing process moves into the gravity-driven regime, as the thickening process will be

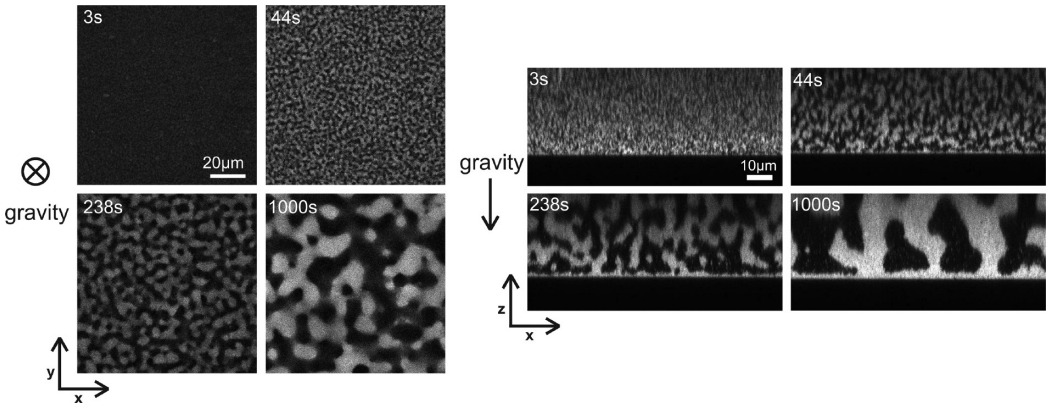

Figure 3. CSLM images at 63× magnification of sample 1 in the (left) *xy* and (right) *xz* planes.

additionally influenced by gravity. We now consider how the presence of a surface affects the phase separation for each of these cases.

In Figure 3, one can see the development of the spinodal decomposition of sample 1 in the vicinity of a single wall. The image sequence one the left is for the *xy* plane (parallel to the surface at a distance from the wall of approximately 40 μm), and that on the right is for the *xz* plane (perpendicular to the surface). (Note that the interconnectivity between domains is more obvious in the *xy* plane than the *xz* plane because of a difference in image depth.) Immediately after homogenization (3 s), the sample is reasonably uniform. As the phase separation progresses, in the *xy* plane, one can see the domains coarsen in a symmetrical network (44−1000 s). In the *xz* plane, it is clear that the liquid (bright) phase preferentially wets the wall, breaking the symmetry of the phase separation perpendicular to the surface (44−1000 s). As the system coarsens, this wetting layer thickens, and a region next to the wetting layer depleted of the liquid phase forms (the depletion layer). The bulk domains grow larger and remain connected to the wetting layer, allowing the wetting phase to be transported to the surface through the spinodal network. As the spinodal structures coarsen, the connecting tubes thicken both parallel and perpendicular to the surface. In the final image (1000 s), the domains are large, the wetting layer is thick, and there are large tubes connecting the bulk liquid phase to the wetting layer.

Figure 4 depicts the phase separation of a system similarly affected by a solid surface, but with demixing in bulk through the nucleation and growth mechanism (sample 2). Initially, the system is homogeneous, but because of the preferential wetting of the surface by the liquid phase, the formation of both wetting and depletion layers occurs quickly (9 s). The wetting layer is distinctly visible much earlier than for sample 1, possibly because of the better contrast between the wetting layer and the bulk. The material outside the vicinity of the surface forms droplets, which generally coarsen by coalescence, as observed in bulk demixing (292−1448 s). The growth of the wetting layer is limited by the droplets diffusing across the depletion layer and coalescing on its surface. These droplets then spread out across the whole wetting layer.

Finally, we consider the separation of sample 3, which demixes through spinodal decomposition similarly to sample 1, although there is significantly less colloidal liquid phase within the system. Initially, one can see a homogenized mixture and little domain growth (Figure 5; 1.7s). The wetting layer is established quickly, the bulk system coarsens through spinodal decomposition, and the wetting layer is connected to bulk domains (63 s). However, as the domains grow and the wetting and depletion layers widen, the domains connecting the bulk to the wetting layer snap as the lack of liquid phase in the depletion region violates the bicontinutiy condition[40] (285 and 1240 s). Away from the wall, in the bulk, the spinodal network remains interconnected/bicontinuous. This behavior significantly differs from the bulk phase separation that holds a bicontinuous network structure until it crosses into the gravity-driven regime (Figure 2). Once the connection between bulk domains and the wetting layer is broken, the wetting layer can grow only by the diffusion of liquid phase across the depletion layer. For sample 3, it is thus apparent that the surface field modifies the bicontinuous structure.

As the samples demixed in the vicinity of a surface, we observed the development of wetting and depletion layers as the structures coarsen. We quantify these observations in average intensity plots in Figure 6. In the *z* direction, the origin represents the position of the solid surface as located by the image analysis described in section 2. In panels a and b of Figure 6, we compare the intensity fluctuations of sample 1 across the *xy* and *xz* planes. In the *y*

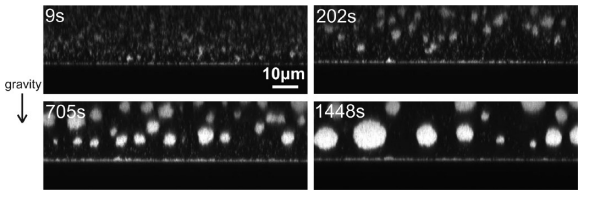

Figure 4. CSLM images showing the progression of the demixing of sample 2.

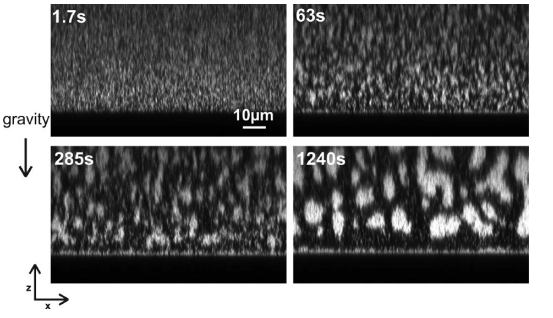

Figure 5. CSLM images of the phase separation of sample 3 in the *xz* plane.

dx.doi.org/10.1021/jp207250q |*J. Phys. Chem. B* 2011, 115, 13168–13174

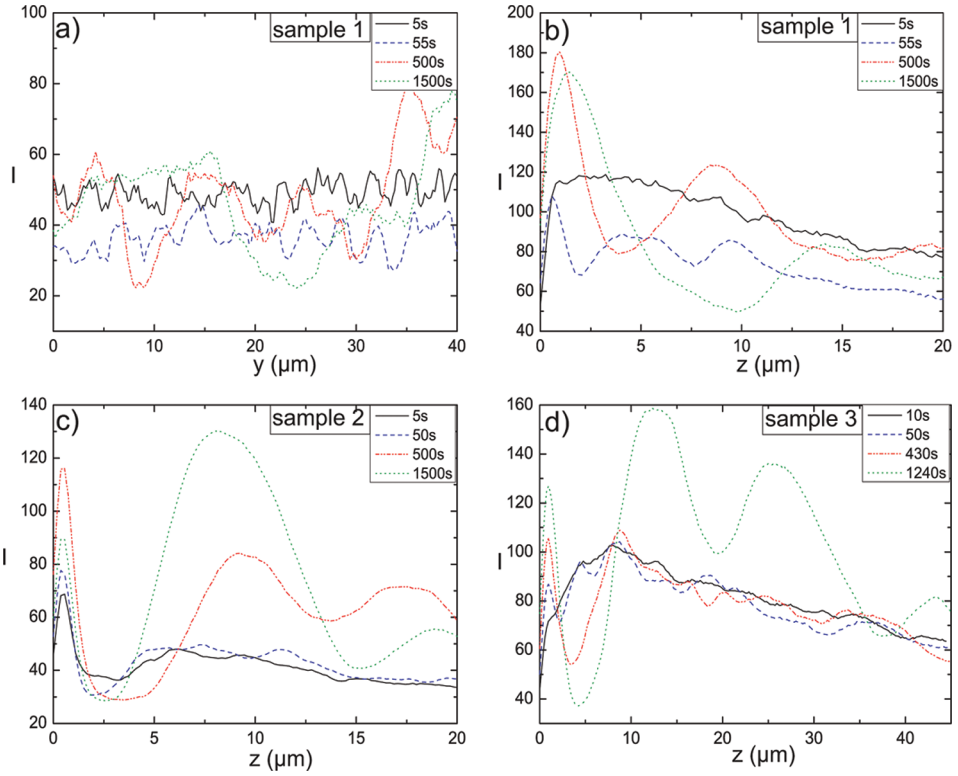

Figure 6. Average intensity per row versus distance in the (a) y and (b) z directions for sample 1, (c) z direction for sample 2, and (d) z direction for sample 3.

direction, the fluctuations are of similar phase and amplitude across the area examined, and they grow in size as domains coarsen. In the z direction, the symmetry of the intensity fluctuations is broken by the presence of the wall. One can observe the growth of an oscillating wave originating from the surface, with first a peak representing the wetting layer, followed by a trough corresponding to the depletion layer. Although the signal becomes noisier with increasing z, the wave breaks down as one moves toward bulk domains. At early times, the oscillations are small, growing in wavelength and amplitude as the system coarsens and the wetting and depletion layers thicken. Similar patterns are observed in panels c and d of Figure 6 for samples 2 and 3, respectively.

We analyzed the wetting-layer thickness (l) as described in section 2 and plot wetting-layer thickness against time for each sample in Figure 7a. The wetting layer grows fastest in sample 1, where bulk domains remain connected to the surface throughout. The wetting layer in sample 2 thickens much more slowly, as growth is limited by the diffusion of droplets across the depletion region and reaches what we assume to be its equilibrium thickness after around 300 s. In sample 3, although the initial layer of liquid wetting the surface is thinner, the wetting layer grows at a rate similar to that of sample 1 for around 200 s. After this time, corresponding to the snap-off of the connecting domains, the growth of the wetting layer slows considerably. This means that the wetting layer is unable to thicken through the faster hydrodynamic mechanism and tends toward the slower diffusion-limited mechanism exhibited by sample 2.

A number of experimental and simulated systems in the diffusive spinodal regime undergoing SDSD have exhibited wetting-layer thickening as $l(t) \sim t^{1/3}$.[7,9,10,14,41,42] In Figure 7b, we plot the wetting-layer growth of each sample against $t^{1/3}$. For sample 1, we obtain a relatively straight line, as indicated, demonstrating that the wetting-layer growth proceeds with an approximate power law of $l(t) \propto t^{1/3}$. The growth in sample 2 clearly does not follow this power law. In sample 3, the wetting-layer growth obeys the power law $l(t) \propto t^{1/3}$ for only the first 200 s.

Images of sample 1 and sample 3 at early times (see Figures 3 and 4) show structures with sharp interfaces connecting bulk domains to the wetting layer, suggesting that wetting-layer growth should be in a hydrodynamic regime.[21,43] Simulations including hydrodynamic effects have shown the wetting layer in this case to grow with an exponent of 1,[11,13,44−46] which has been observed experimentally in a binary liquid system.[22] The crossover between diffusive and hydrodynamic growth exponents in the wetting layer has been observed in simulation;[11,13,44,45] however, this might not occur at the same time as the crossover between the diffusive and hydrodynamic regimes in the bulk.[45] We plot our data against known exponents rather than interpretting it using, for example, log−log plots, as the prescence of a slow crossover could lead to misleading results over a short time scale.

In our experiments, some curvature at early times in plots of the growth of the bulk domain length scale in Figure 2 indicates that samples 1 and 3 are in the process of crossing over from the diffusive to the hydrodynamic regime in the bulk. These slow crossovers have been observed in similar systems.[35,39] It appears that the crossover from $\sim t^{1/3}$ to t^1 growth occurs at a later time for the wetting layer in our system than in the bulk and, therefore, grows with a diffusive exponent despite the presence of sharp interfaces. This is likely due to increased friction at the wall, a factor that also accounts for the larger width of domains compared to the wetting layer.[11,45] The acceleration of wetting-layer growth at late times in sample 1 suggests that the crossover

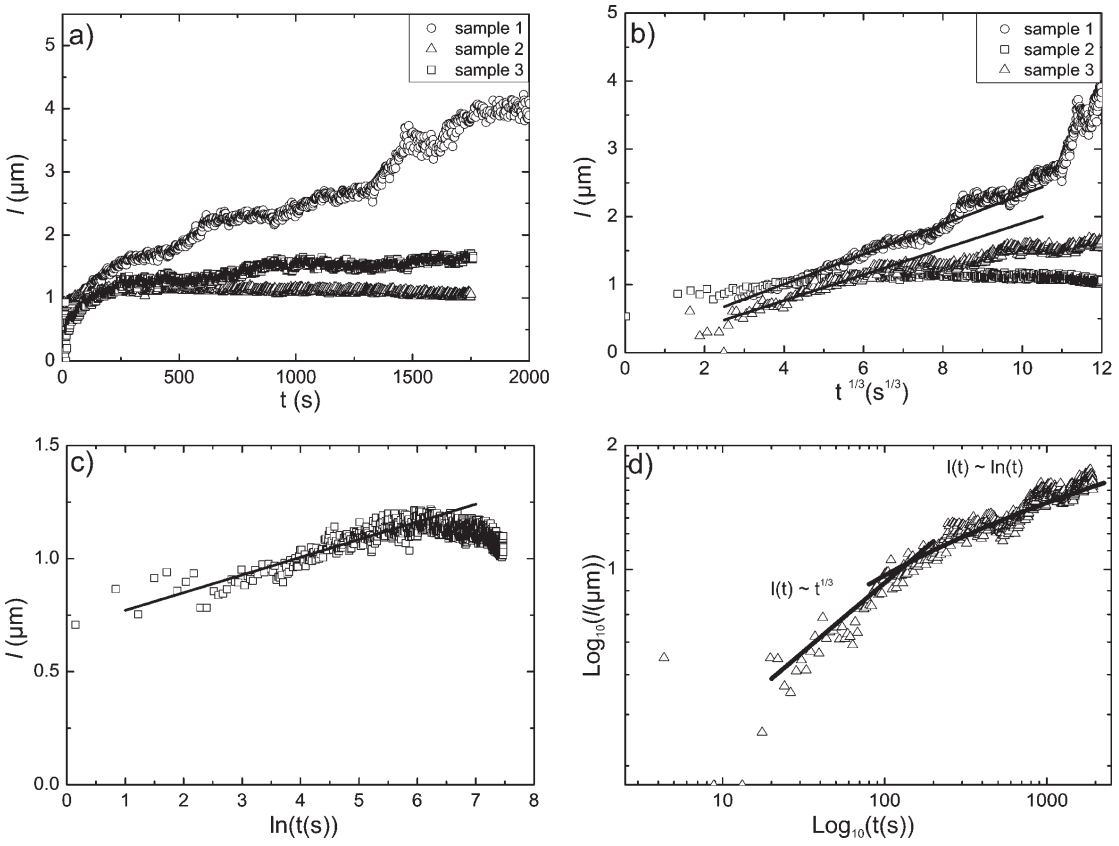

Figure 7. (a) Plot of wetting-layer thickness versus time for samples 1−3. (b) Wetting-layer growth for each sample versus $t^{1/3}$. The thick black lines represent linear fits to the data. (c) Plot of wetting-layer growth versus $\ln(t)$ for sample 2. The thick black line represents a linear fit to the data. (d) Double logarithmic plot of wetting-layer thickness versus time for sample 3.

to the hydrodynamic regime is beginning. Additionally, we note that a sample with a lower-viscosity solvent that had crossed over more fully into the hydrodynamic regime exhibited a growth exponent closer to 1. The time scale of this separation was too fast for detailed measurement.

The wetting layer in sample 2 grows much more slowly as it is limited by the diffusion of liquid droplets across the depletion layer. After around 300 s, it stops growing as it reaches its equilibrium thickness, determined by the interplay between gravitational forces and the depletion interaction.[47] Because of the relative densities of the liquid and gas phases, once bulk demixing moves into the gravity-driven regime, we expect liquid droplets to fall onto the wetting layer and a macroscopic interface to form.[21,37] Our experiments were stopped before this, and we expect that the droplets studied in these experiments were too small to have been significantly affected by sedimentation. From the numerical simulations of Puri and Binder[18] and Yan and Xie,[17] the predicted growth law is dependent, among other factors, on the strength of surface potential and quench depth. These properties are difficult to evaluate in an experiment, but $l(t) \sim \ln(t)$ is predicted under certain conditions and has been observed in polymer experiments.[48] From Figure 7c, it appears that a logarithmic law applies before the equilibrium thickness is attained.

For sample 3, we observed that, initially, while the bulk domain remained connected to the wetting layer, it grew with a power law of approximately $l(t) \sim t^{1/3}$ (Figure 7b). We explain the diffusive growth exponent with an argument similar to that used for sample 1. Once the domains snap off after around 200 s, growth slows as the thickening of the wetting layer becomes limited by the diffusion of the liquid phase across the depletion layer, the growth mechanism observed for sample 2, and a logarithmic growth law could apply. The diffusion of the partially interconnected domains to the wetting layer will, however, be different from that of spherical drops in sample 2. We illustrate this crossover between regimes in Figure 7d. Both the crossover between the two different mechanisms, which might occur later than in the bulk, and the morphology of the demixing structure close to the wall and its connectivity to the wall should be considered when considering the role of hydrodynamics.

4. CONCLUSIONS

We have investigated the effect of a solid surface on the fluid−fluid demixing of a colloid−polymer mixture. Using the technique of CSLM, we obtained real-space images of the phase separation in the directions parallel and perpendicular to the surface, demonstrating that the surface field breaks the symmetry of the phase-separating morphology and influences the coarsening behavior of domains. We have studied the growth of the wetting layer for systems of differing composition, obtaining results in accordance with previous experiments and simulations. The prediction of a growth law for a particular experimental system remains challenging because of the involvement of a high number of competing influences. The role of hydrodynamics in wetting-layer evolution has been widely discussed, and we

illustrate that the hydrodynamic transport of the wetting phase from the bulk domains to the surface leads to accelerated growth of the wetting layer. We found that the demixing structure remained bicontinuous in the bulk, but disconnected from the wall, a phenomenon that has a strong effect on both the morphology and kinetics of the phase separation. Additionally, we considered the crossover between the diffusive and hydrodynamic regimes, which occurs at a later time at the wetting layer than in the bulk. This resulted in a purely diffusive growth exponent for the wetting layer, whereas bulk domains were crossing over between regimes. Finally, interfacial fluctuations might play an additional role,[28,47] a possibility that we plan to study in the future.

AUTHOR INFORMATION

Corresponding Author

*E-mail: Elizabeth.Jamie@chem.ox.ac.uk.

REFERENCES

(1) Bray, A. J. *Adv. Phys.* **1994**, *43*, 357.
(2) Binder, K. *Rep. Prog. Phys.* **1987**, *50*, 783.
(3) Tanaka, H. *J. Phys.: Condens. Matter* **2001**, *13*, 4637.
(4) de Gennes, P. G.; Brochard-Wyrat, F.; Quéré, D. *Capillarity and Wetting Phenomena: Drops, Bubbles, Pearls, Waves*; Springer: Berlin, 2004.
(5) Ball, R. C.; Essery, R. L. H. *J. Phys.: Condens. Matter* **1990**, *2*, 10303.
(6) Jones, R. A. L.; Norton, L. J.; Kramer, E. J.; Bates, F. S.; Wiltzuis, P. *Phys. Rev. Lett.* **1991**, *66*, 1326.
(7) Brown, G.; Chakrabarti, A. *Phys. Rev. A* **1992**, *46*, 4829.
(8) Puri, S.; Binder, K. *Phys. Rev. E* **1994**, *49*, 5359.
(9) Krausch, G.; Dai, C.-A.; Kramer, E. J.; Bates, F. S. *Phys. Rev. Lett.* **1993**, *71*, 3669.
(10) Puri, S.; Binder, K. *Phys. Rev. A* **1992**, *46*, 4487.
(11) Marko, J. F. *Phys. Rev. E.* **1993**, *48*, 2861.
(12) Geoghegan, M.; Nicolai, T.; Penforld, J.; Jones, R. A. L. *Macromolecules* **1997**, *30*, 4220.
(13) Tanaka, H.; Araki, T. *Europhys. Lett.* **2000**, *51*, 154.
(14) Straub, W.; Bruder, F.; Brenn, R.; Krausch, G.; Bielefeldt, H.; Kirsch, A.; Marti, O.; Mlynek, J. L.; Marko, J. F. *Europhys. Lett.* **1995**, *29*, 353.
(15) Yan, L.-T.; Xie, X.-M. *Macromolecules* **2006**, *39*, 2388.
(16) Puri, S.; Binder, K. *Phys. Rev. E* **2002**, *66*, 061602.
(17) Yan, L.-T.; Xie, X.-M. *J. Chem. Phys.* **2007**, *126*, 064908.
(18) Puri, S.; Binder, K. *Phys. Rev. Lett.* **2001**, *86*, 1797.
(19) Yan, L.-T.; Xie, X.-M. *Polymer* **2006**, *47*, 6472.
(20) Puri, S.; Binder, K. *Phys. Rev. E* **1993**, *49*, 6.
(21) Siggia, E. D. *Phys. Rev. A* **1979**, *20*, 595.
(22) Guenoun, P.; Beysens, D.; Robert, M. *Physica A* **1991**, *172*, 137.
(23) Wiltzuis, P.; Cumming, A. *Phys. Rev. Lett.* **1991**, *66*, 3000.
(24) Bastea, S.; Puri, S.; Lebowitz, J. *Phys. Rev. E* **2001**, *63*, 041513.
(25) Asakura, S.; Oosawa, F. *J. Polym. Sci.* **1958**, *33*, 158.
(26) Vrij, A. *Pure Appl. Chem.* **1976**, *48*, 471.
(27) Aarts, D. G. A. L.; Schmidt, M.; Lekkerkerker, H. N. W. *Science* **2004**, *304*, 807.
(28) Hennequin, Y.; Aarts, D. G. A. L.; Indekeu, J. O.; Lekkerkerker, H. N. W.; Bonn, D. *Phys. Rev. Lett.* **2008**, *100*, 178305.
(29) Aarts, D. G. A. L.; Dullens, R. P. A.; Lekkerkerker, H. N. W.; Bonn, D.; van Roij, R. *J. Chem. Phys.* **2004**, *120*, 1973.
(30) OPTIM Glycerine: Physical Properties, Dow Corning. http://www.dow.com/glycerine/resources/physicalprop.htm (accessed June 2011).
(31) Kumacheva, E.; Kalinina, O.; Lilge, L. *Adv. Mater.* **1999**, *11*, 231.
(32) Koenderink, G. H.; Aarts, D. G. A. L.; De Villeneuve, V. W. A.; Philipse, A. P.; Tuiner, R.; Lekkerkerker, H. N. W. *Biomacromolecules* **2003**, *4*, 129.
(33) Jamie, E. A. G.; Davies, G. J.; Howe, M. D.; Dullens, R. P. A.; Aarts, D. G. A. L. *J. Phys.: Condens. Matter* **2008**, *20*, 494231.
(34) Jamie, E. A. G.; Wensink, H. H.; Aarts, D. G. A. L. *Soft Matter* **2010**, *6*, 250.
(35) Jamie, E. A. G.; Dullens, R. P. A.; Aarts, D. G. A. L. *J. Phys.: Condens. Matter* **2011**, *23*, 194115.
(36) Hashimoto, T.; Koga, T.; Jinnia, H.; Nishikawa, Y. *Nuovo Cim.* **1998**, *20*, 1947.
(37) Aarts, D. G. A. L.; Dullens, R. P. A.; Lekkerkerker, H. N. W. *New. J. Phys* **2005**, *7*, 40.
(38) Hell, S.; Reiner, G.; Cremer, C.; Stelzer, E. H. K. *J. Microsc.* **1993**, *169*, 391.
(39) Bailey, A. E.; Poon, W. C.; Christianson, R. J.; Schofield, A. B.; Gasser, U.; Prasad, V.; Manley, S.; Segre, P. N.; Cipelletti, L.; Meyer, W. V.; Doherty, M. P.; Sankaran, S.; Jankovsky, A. L.; Shiley, W. L.; Bowen, J. P.; Eggers, J. C.; Kurta, C.; Lorik, T., Jr.; Pusey, P. N.; Weitz, D. A. *Phys. Rev. Lett.* **2007**, *99*, 205701.
(40) Onuki, A. *Europhys. Lett.* **1994**, *28*, 175.
(41) Krausch, G.; Dai, C.-A.; Kramer, E. J.; Marko, J. F.; Bates, F. S. *Macromolecules* **1993**, *26*, 5566.
(42) Steiner, U.; Klien, J. *Phys. Rev. Lett.* **1996**, *77*, 2526.
(43) Bray, A. J. Coarsening dynamics of nonequilibrium phase transitions. In *Soft and Fragile Matter: Nonequilibrium Dynamics, Metastability and Flow*; Cates, M. E., Evans, M. R., Eds.; Taylor & Francis: London, 2000; pp 205−258.
(44) Jaiswal, P. K.; Puri, S.; Das, S. K. Hydrodynamic Crossovers in Surface-Directed Spinodal Decomposition and Surface Enrichment, 2011. *arXiv:1011.6297.v1 [cond-mat.soft]*. arXiv.org e-Print archive. http://arxiv.org/abs/1011.6297 (accessed June 2011).
(45) Chen, H.; Chakrabarti, A. *Phys. Rev. E* **1997**, *55*, 5680.
(46) Tanaka, H. *Phys. Rev. Lett.* **1993**, *70*, 2770.
(47) Indekeu, J. O.; Aarts, D. G. A. L.; Hennequin, Y.; Lekkerkerker, H. N. W.; Bonn, D. *Phys. Rev. E.* **2010**, *81*, 041604.
(48) Geoghegan, M.; Ermer, H.; Jüngst, G.; Krausch, G.; Brenn, R. *Phys. Rev. E* **2000**, *62*, 940.